SCIENCE CHINA
Information Sciences

• MOOP •

April 2022, Vol. 65 144201:1–144201:3
https://doi.org/10.1007/s11432-020-3222-2

Distributed unmanned flocking inspired by the collective motion of pigeon flocks

Huaxin QIU, Qingrui ZHOU, Changhao SUN* & Xiaochu WANG

Qian Xuesen Laboratory of Space Technology, China Academy of Space Technology, Beijing 100094*, China*

Received 25 September 2020/Revised 29 December 2020/Accepted 26 February 2021/Published online 16 March 2022

Citation Qiu H X, Zhou Q R, Sun C H, et al. Distributed unmanned flocking inspired by the collective motion of pigeon flocks. Sci China Inf Sci, 2022, 65(4): 144201, https://doi.org/10.1007/s11432-020-3222-2

An unmanned aerial vehicle (UAV) swarm system outperforms a single UAV in terms of performance, reliability, adaptability, and economy by concentrating resources and utilizing complementing advantages [1]. For example, by flexibly configuring single-plane loads such as reconnaissance detection, electronic jamming, and fire strikes in the swarm, real-time reconnaissance and strikes on weak parts of key targets will be carried out. According to a theoretical and empirical study on the autonomous coordinated flocking of the UAV swarm system, the distributed decision-making problem is expected to be solved [2–5]. Researchers of bird flock behaviors have been concerned about such a problem for a long time. The mechanism observed in bird flocks inspires the design of UAV-flocking control methods [2–5]. However, the abovementioned methods [2–5] apply only to homogeneous groups or groups with a single leader and cannot be applied to the UAV flocking control problem under multiple dominant individual conditions. To solve this problem, this study proposes the application of a UAV flocking control algorithm to a heterogeneous swarm with multiple dominant individuals by studying the mechanism of the collective motion of pigeon flocks. Collective motion is the group behavior of birds, mammals, fishes, insects, and other social organisms that, after long-term evolution, are adapted according to the living environment. Researchers favor pigeons to study collective motion because of their ease of breeding and observation. Individuals follow simple local interaction rules to form a highly ordered collective motion in the homing flight of a pigeon flock with multiple dominant individuals and swarm intelligence emerges at the group level [6]. When flying along a smooth trajectory, individuals tend to follow the average flight direction of their neighbors. When suddenly turning, they will tend to follow their leader. Although qualitative analysis makes the pigeon swarm intelligence mechanism gradually comprehensive, obstacles are encountered when investigating the simple rules behind pigeon flocks' orderly movement owing to the lack of a clear description of interaction patterns and switching relationships.

Dual-pattern mechanism of pigeon flocks. The homing flight data of the pigeons analyzed herein are derived from hf2 in [7]. To obtain the quantitative relationship between trajectory curvature and interaction patterns, the frequency of different spacings between pigeons and their leaders under different group curvatures in different interaction patterns is counted. After retaining about 80% of the data by filtering low-frequency data, insets (i) and (ii) in Figure 1(a) are plotted to show the frequency distributions of the egalitarian (78.96%) and hierarchical (77.95%) interaction patterns, respectively, and the higher is the frequency, the darker is the color of the corresponding square in insets (i) and (ii). Note that the curvature division has an accuracy of 0.0001 m^{-1}, whereas the spacing division has an accuracy of 0.5 m^{-1}. The maximum spacing in the hierarchical interaction pattern (22.5 m^{-1}) is greater than that in the egalitarian interaction pattern (16.5 m^{-1}), as shown using black frames in the insets (i) and (ii). After counting the frequency of different interaction patterns under different group curvatures in the remaining data, the percentage of hierarchical interaction patterns varying with trajectory curvature is calculated. The percentage of hierarchical interaction patterns roughly increases in an S-shape with the group trajectory curvature shown by the dotted line in Figure 1(a).

Collective motion model of the pigeon flocks. The homing flight of pigeon flocks is established using a collective motion model on the above-described dual-pattern mechanism. The unique characteristics of the proposed model can be observed in the quantitative description of the switching relationship between the two interactive patterns of pigeon flocks. Because this study only discusses the motion law of N pigeons within D-dimensional Euclidean space, each individual is considered a particle, and its dynamic model is shown in the following second-order agent model [8]:

$$\begin{cases} \dot{\boldsymbol{x}}_i = \boldsymbol{v}_i, \\ \dot{\boldsymbol{v}}_i = \boldsymbol{u}_i, \end{cases} \tag{1}$$

where the index of pigeon $i = 1, \ldots, N$ and $\boldsymbol{x}_i, \boldsymbol{v}_i, \boldsymbol{u}_i \in \mathbb{R}^{D\times 1}$ represent the position vector, velocity vector, and control input vector of i, respectively.

The probability p_{h} that the pigeon flock adopts the hier-

* Corresponding author (email: sunchanghao@qxslab.cn)

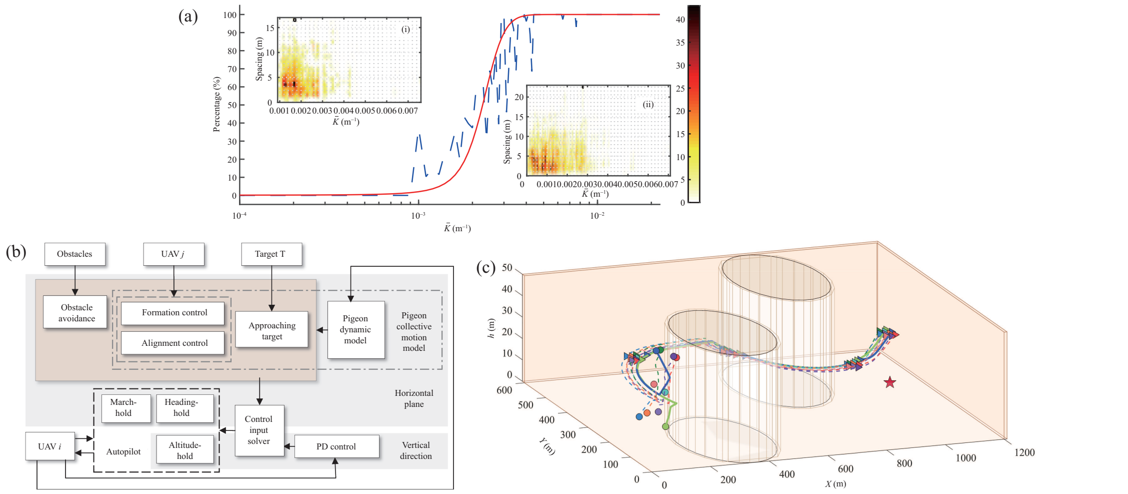

Figure 1 (Color online) Unmanned aerial vehicle flocking inspired by pigeons. (a) Percentage change of hierarchical interaction patterns; (b) UAV flocking framework; (c) simulation results.

archical interaction pattern is defined as follows:

$$p_{\mathrm{h}} = 1/\left(1 + \alpha \mathrm{e}^{-\beta \bar{K}^t}\right), \tag{2}$$

where $\alpha > 1$ and $\beta > 0$ are logistic function parameters, and $\bar{K}^t$ is the group trajectory curvature at time t. The set of individuals with the location information of target T is defined as the set S_{d} of dominant individuals.

Based on the above definition, individuals will generate control vector $\boldsymbol{u}_i$ based on neighbor interaction information and target locations to synchronize with neighbors, maintain a desired distance from the neighbors, and reach the target position vector $\boldsymbol{x}_{\mathrm{T}}$ with a maximum allowable error.

$$\boldsymbol{u}_i = \begin{cases} -K^{\mathrm{F}} \sum\limits_{j \in \mathcal{N}_i^1} \nabla_{\boldsymbol{x}_i} V_{ij}^{\mathrm{F}} \left(\|\boldsymbol{x}_{ij}\|\right) \\ -K^{\mathrm{T}} \nabla_{\boldsymbol{x}_i} V_i^{\mathrm{T}} \left(\|\boldsymbol{x}_i - \boldsymbol{x}_{\mathrm{T}}\|\right) & i \in S_{\mathrm{d}}, \\ -K^{\mathrm{V}} w \sum\limits_{j \in \mathcal{N}_i} \boldsymbol{v}_{ij}, \\ -K^{\mathrm{F}} \sum\limits_{j \in \mathcal{N}_i^1} \nabla_{\boldsymbol{x}_i} V_{ij}^{\mathrm{F}} \left(\|\boldsymbol{x}_{ij}\|\right) & i \notin S_{\mathrm{d}}, \\ -K^{\mathrm{V}} \left(\sum\limits_{j \in \mathcal{N}_i \backslash S_{\mathrm{d}}} \boldsymbol{v}_{ij} + w \sum\limits_{j \in \mathcal{N}_i \bigcap S_{\mathrm{d}}} \boldsymbol{v}_{ij} \right), \end{cases} \tag{3}$$

where $K^{\mathrm{F}} > 0$, $K^{\mathrm{T}} > 0$, and $K^{\mathrm{V}} > 0$ represent the formation, target, and alignment control gains, respectively. $\mathcal{N}_i^1$ and $\mathcal{N}_i^2 \subseteq \mathcal{N}_i^1$ represent the neighbor sets in the egalitarian and hierarchical interaction patterns, respectively. $\boldsymbol{x}_{ij} = \boldsymbol{x}_i - \boldsymbol{x}_j$ and $\boldsymbol{v}_{ij} = \boldsymbol{v}_i - \boldsymbol{v}_j$ represent the position and velocity vectors of individual i relative to individual j, respectively. When the pigeon flock adopts the egalitarian interaction pattern, the current neighbor set is $\mathcal{N}_i = \mathcal{N}_i^1$ and the alignment weight is $w = 1$; otherwise, $\mathcal{N}_i = \mathcal{N}_i^2$ and $w = w'$, where $w' \geqslant 1$ represents the alignment weight in the hierarchical interaction pattern. $V_{ij}^{\mathrm{F}}\left(\|\boldsymbol{x}_{ij}\|\right)$ and $V_i^{\mathrm{T}}\left(\|\boldsymbol{x}_i - \boldsymbol{x}_{\mathrm{T}}\|\right)$ represent the potential field functions of the formation and the target, respectively.

UAV flocking algorithm based on the pigeon collective motion model. To realize the autonomous coordination of a UAV swarm with multiple dominant individuals, a distributed algorithm (Algorithm 1) is proposed that maps the collective motion model of pigeon flocks to the UAV flocking control. The UAV flocking control is decoupled into horizontal plane and vertical direction control, as shown in Figure 1(b). On the horizontal plane, each UAV not only performs flock formation, flock alignment, and target approach based on the collective motion model of pigeon flocks but also evades obstacles. Each UAV attempts to remain at the desired altitude h_{exp} in a vertical direction. The probability p_{h} that each UAV adopts a hierarchical interaction pattern is estimated using (2), which is inspired by the pigeon collective motion model. Owing to the limitations of information acquisition in the distributed framework, the actual group trajectories $\bar{K}$ adopted by the UAVs are $|\sum_{j \in \mathcal{N}_i} K_i| / |\mathcal{N}_i|$, where $|A|$ represents the number of elements in set A. The detailed Algorithm 1 is as follows.

Step 1. Consider the current coordinate $[X_i, Y_i]'$ of UAV i as the position vector $\boldsymbol{x}_i$ of pigeon i. Consider the current horizontal airspeed component $[V_i \cos\psi_i, V_i \sin\psi_i]'$ of UAV i at t on the X- and Y-axes as the velocity vector $\boldsymbol{v}_i$ of pigeon i, where V_i and ψ_i represent the horizontal velocity and yaw angle of UAV i, respectively. Based on the above settings, UAV dynamics is transformed into the second-order agent model similar to that of pigeons. Then, based on the probability p_{h}, the egalitarian or hierarchical interaction pattern is selected. The corresponding current neighbor set $\mathcal{N}_i$ and alignment weight w of pigeon i are generated according to the selected pattern.

Step 2. Calculate the current control input vector $\boldsymbol{u}_i$ of pigeon i using the following equation:

$$\boldsymbol{u}_i = \begin{cases} -K^{\mathrm{F}} \sum\limits_{j \in \mathcal{N}_i^1} \nabla_{\boldsymbol{x}_i} V_{ij}^{\mathrm{F}} \left(\|\boldsymbol{x}_{ij}\|\right) \\ -K^{\mathrm{O}} \sum\limits_{j=1}^{N_{\mathrm{O}}} \nabla_{\boldsymbol{x}_i} V_i^{\mathrm{O}} \left(\left\|\boldsymbol{x}_i - \boldsymbol{x}_j^{\mathrm{O}}\right\|\right) & i \in S_{\mathrm{d}}, \\ -K^{\mathrm{T}} \nabla_{\boldsymbol{x}_i} V_i^{\mathrm{T}} \left(\|\boldsymbol{x}_i - \boldsymbol{x}_{\mathrm{T}}\|\right) \\ -K^{\mathrm{V}} w \sum\limits_{j \in \mathcal{N}_i} \boldsymbol{v}_{ij}, \\ -K^{\mathrm{F}} \sum\limits_{j \in \mathcal{N}_i^1} \nabla_{\boldsymbol{x}_i} V_{ij}^{\mathrm{F}} \left(\|\boldsymbol{x}_{ij}\|\right) \\ -K^{\mathrm{O}} \sum\limits_{j=1}^{N_{\mathrm{O}}} \nabla_{\boldsymbol{x}_i} V_i^{\mathrm{O}} \left(\left\|\boldsymbol{x}_i - \boldsymbol{x}_j^{\mathrm{O}}\right\|\right) & i \notin S_{\mathrm{d}}, \\ -K^{\mathrm{V}} \left(\sum\limits_{j \in \mathcal{N}_i \backslash S_{\mathrm{d}}} \boldsymbol{v}_{ij} + w \sum\limits_{j \in \mathcal{N}_i \cap S_{\mathrm{d}}} \boldsymbol{v}_{ij} \right), \end{cases} \tag{4}$$

where $K^{\mathrm{O}} > 0$ represents the obstacle avoidance gain,

$j = 1, \ldots, N_{\rm O}$, $N_{\rm O}$ represents the number of obstacles, $V_i^{\rm O}(\|\boldsymbol{x}_i - \boldsymbol{x}_j^{\rm O}\|)$ represents the potential field function for obstacles, and $\boldsymbol{x}_j^{\rm O} = [X_j^{\rm O}, Y_j^{\rm O}]'$ represents the horizontal position vector of the point closest to UAV i on the surface of obstacle j.

Step 3. Generate current control input $u_{\rm h}$ in the vertical direction using the following equation:

$$u_{\rm h} = -K^{\rm P}\left(h_i - h_{\rm exp}\right) - K^{\rm D}\zeta_i, \tag{5}$$

where $K^{\rm P} > 0$ and $K^{\rm D} > 0$ represent the proportion and differential control gains in the vertical direction respectively, and h_i and ζ_i represent the altitude and altitude rate of UAV i, respectively.

Step 4. Produce the current autopilot control input $\left(V_{\rm C}^i, \psi_{\rm C}^i, h_{\rm C}^i\right)$ of UAV i using the following equation:

$$\begin{cases} V_{\rm C}^i = \tau_{\rm V}\left(\boldsymbol{u}_i^1 \cos\psi_i + \boldsymbol{u}_i^2 \sin\psi_i\right) + V_i, \\ \psi_{\rm C}^i = \tau_\psi\left(\boldsymbol{u}_i^2 \cos\psi_i - \boldsymbol{u}_i^1 \sin\psi_i\right)/V_i + \psi_i, \\ h_{\rm C}^i = h_i + \left(\tau_{\rm a} + \tau_{\rm b}\right)\xi_i + \tau_{\rm a}\tau_{\rm b}u_{\rm h}, \end{cases} \tag{6}$$

where $\tau_{\rm V}$, τ_ψ, and $(\tau_{\rm a}, \tau_{\rm b})$ and $V_{\rm C}^i$, $\psi_{\rm C}^i$, and $h_{\rm C}^i$ represent the time constants and control inputs of three autopilots: the march-, heading-, and altitude-hold autopilots, respectively. Calculate UAV states $(X_i, Y_i, h_i, V_i, \psi_i, \zeta_i)$ at the next time by the UAV model presented in [3].

Simulation results. A swarm of 10 UAVs is assigned to reach the target as a whole in an environment with obstacles. The activity range of UAVs is limited to a space of 1200 m $\times$ 600 m $\times$ 100 m ($l \times w \times h$) dimensions. In the UAV swarm's direction of target approach, i.e., $\boldsymbol{x}_{\rm T} = [1100\ {\rm m}, 400\ {\rm m}]'$, there are two 100-m-high cylindrical obstacles. These two obstacles have a radius of 150 m^{-1}, and their centers are $[350\ {\rm m}, 150\ {\rm m}]'$ and $[350\ {\rm m}, 150\ {\rm m}]'$, respectively. UAVs 4 and 8 are set as dominant individuals equipped with the location information of the target T. The UAV swarm must fly to a position 25-m-high above the target.

Each UAV autonomously controls itself based on Algorithm 1. The parameters of Algorithm 1 are set as follows: N= 10, $\tau_{\rm V} = 3$ s; $\tau_\psi = 0.75$ s; $\tau_{\rm a} = 1/3$ s; $\tau_{\rm b} = 3$ s; D= 2; $\alpha = 1000$; $\beta = 65$; $S_{\rm d} = \{4, 8\}$; $h_{\rm exp} = 25$ m; $K^{\rm F} = 1.8$; $K^{\rm V} = 0.6$; $K^{\rm T} = 0.1$; $K^{\rm P} = 100$; $K^{\rm D} = 10$; and w'= 6.5. Note that the UAV activity boundary is treated as an obstacle herein. The obstacle avoidance gains $K^{\rm O}$ of the cylindrical obstacles and the activity boundary are 5 and 1000, respectively.

Figure 1(c) depicts the simulation results of UAV flocking based on Algorithm 1 under the obstacle environment. In Figure 1(c), the UAV activity range is marked using a rectangular fence, and the target T is marked using a pentagon. The surfaces outside the cylinders mark the areas with the minimum allowable distance from the obstacles, and the obstacles are marked using cylinders. The trajectories of dominant and ordinary UAVs are marked using heavy solid lines and thin dotted lines, respectively. The initial position of the UAV is marked using solid circles, and its positions at 20-s intervals are marked using solid triangles. Based on Algorithm 1, the UAV swarm could gradually converge to the same altitude and reach the target as a whole without clustering, as shown in Figure 1(c).

Conclusion. The contribution of this study is mainly reflected in the following three aspects. (1) In the study on pigeon flock mechanisms, only the qualitative analysis of pigeon flocks using dual interaction patterns is available. This study gives the quantitative relationship between the interaction pattern of pigeon flocks and the curvature of group trajectories; additionally, an S-shaped curve of interaction pattern switching is obtained from the practical data of pigeon flocks. (2) Although the collective motion model is actively researched, the majority of the models are homogeneous and single-mode. By describing the interaction pattern switching and dominant individuals based on the quantitative relationship of pattern switching in pigeon flocks, herein, a heterogeneous and multi-modal collective motion model, which can better reflect the characteristics of natural living systems, is established. (3) Coordinating a group of UAVs to cross an obstacle environment when only a few UAVs are equipped with preliminary information related to the obstacle is difficult. Although distributed flocking algorithms can improve the deficient robustness of centralized algorithms, most of the existing distributed algorithms do not consider the difference in UAV capability within the group. Additionally, this study proposed a distributed UAV flocking algorithm that uses the swarm intelligence of pigeon flocks to guide UAV swarms with multiple dominant individuals to synchronously approach a target without collisions. Compared with the traditional distributed algorithm (see Appendix A), Algorithm 1 has better synchronization, faster target approaching speed, and less communication loss because of the interaction pattern switching.

Acknowledgements This work was supported in part by National Natural Science Foundation of China (Grant Nos. 62103414, 62173330) and China Postdoctoral Science Foundation (Grant No. 2020M670410).

Supporting information Videos and other supplemental documents. The supporting information is available online at info.scichina.com and link.springer.com. The supporting materials are published as submitted, without typesetting or editing. The responsibility for scientific accuracy and content remains entirely with the authors.

References

1 Pham H X, La H M, Feil-Seifer D, et al. A distributed control framework of multiple unmanned aerial vehicles for dynamic wildfire tracking. IEEE Trans Syst Man Cybern Syst, 2020, 50: 1537–1548

2 Luo Q, Duan H. Distributed UAV flocking control based on homing pigeon hierarchical strategies. Aerospace Sci Tech, 2017, 70: 257–264

3 Zhang X, Duan H. Altitude consensus based 3D flocking control for fixed-wing unmanned aerial vehicle swarm trajectory tracking. Proc Inst Mech Eng Part G-J Aerospace Eng, 2016, 230: 2628–2638

4 Lwowski J, Majumdar A, Benavidez P, et al. Bird flocking inspired formation control for unmanned aerial vehicles using stereo camera. IEEE Syst J, 2019, 13: 3580–3589

5 Qiu H, Duan H. A multi-objective pigeon-inspired optimization approach to UAV distributed flocking among obstacles. Inf Sci, 2020, 509: 515–529

6 Chen D, Vicsek T, Liu X, et al. Switching hierarchical leadership mechanism in homing flight of pigeon flocks. Euro-phys Lett, 2016, 114: 60008

7 Nagy M, Ákos Z, Biro D, et al. Hierarchical group dynamics in pigeon flocks. Nature, 2010, 464: 890–893

8 Qiu H X, Duan H B, Fan Y M, et al. Pigeon flock interaction pattern switching model and its synchronization analysis (in Chinese). CAAI Trans Intell Technol, 2020, 15: 334–343